

Original Research

# High-Throughput Sequencing to Investigate the Expression and Potential Role of Differentially Expressed microRNAs in Myocardial Cells after Ischemia-Reperfusion Injury

Senjie Li<sup>1</sup>, Dongqing Lv<sup>2</sup>, Yan Lu<sup>1</sup>, Yanwei Zhang<sup>1</sup>, Yongping Jia<sup>1,\*</sup> <sup>1</sup>Department of Cardiology, First Hospital of Shanxi Medical University, 030001 Taiyuan, Shanxi, China<sup>2</sup>Department of Endocrinology, First Hospital of Shanxi Medical University, 030001 Taiyuan, Shanxi, China\*Correspondence: [sdyjyp@126.com](mailto:sdyjyp@126.com) (Yongping Jia)

Academic Editor: Said El Shamieh

Submitted: 27 July 2023 Revised: 2 October 2023 Accepted: 30 October 2023 Published: 23 January 2024

## Abstract

**Background:** microRNAs (miRNAs) are closely associated with the pathogenesis of various diseases, but the relationship between miRNAs and myocardial ischemia-reperfusion (I/R) injury remains unclear. Therefore, we aimed to explore the role and function of miRNAs and identify target genes regulating I/R. **Methods:** We established a hypoxia/reoxygenation (H/R) model to detect differentially expressed miRNAs using high-throughput sequencing in rat myocardial cells. Gene Ontology (GO) and Kyoto Encyclopedia of Genes and Genomes (KEGG) enrichment were used to analyze the potential functions and signaling pathways of target genes. **Results:** We identified 113 differentially expressed miRNAs, comprising 76 and 37 upregulated and downregulated genes, respectively. Database predictions suggested that miR-200a-3p may act through the ferroptosis pathway, and we assessed the expression of miR-200a-3p, iron ions, and ferroptosis markers. The expression of miR-200a-3p significantly increased in the H/R group, along with increased production of reactive oxygen species (ROS) and iron ions. When the expression of miR-200a-3p was inhibited, iron ions and ROS levels decreased significantly. Western blotting showed that transferrin receptor (TFRC) and Acyl-coA synthetase long-chain family member 4 (ACSL4) levels were decreased and Glutathione peroxidase 4 (GPX4) expression was increased. **Conclusions:** These findings offer a novel perspective on I/R regulation, and the specific mechanisms underlying the actions of miR-200a-3p merit further investigation.

**Keywords:** myocardial cells; microRNA; ischemia-reperfusion; high-throughput sequencing; ferroptosis

## 1. Introduction

Cardiovascular diseases seriously endanger human health and are the leading cause of death in humans [1]. Early angioplasty can save the agonal myocardium and reduce myocardial damage in patients with myocardial infarction. Coronary interventions and bypass surgery, performed worldwide, have successfully saved the lives of many patients with myocardial infarction and protected the myocardium to the maximum extent. However, when reperfusion occurs after the opening of an occluded vessel, there is a risk of tissue and organ damage, which is known as ischemia-reperfusion (I/R) injury. This injury can potentially impair myocardial metabolism and ultrastructure, leading to cardiac insufficiency during the later stages of the disease [2,3]. Therefore, early reduction in myocardial ischemia-reperfusion injury (MIRI) merits further mechanistic investigations.

microRNAs (miRNAs) hold immense value in medical research owing to their ease of synthesis and modification. Their roles are not to encode and translate proteins directly but to bind to specific RNAs. They combine with the downstream 3' untranslated regions of mature messenger RNAs (mRNAs) to inhibit mRNA expression and ultimately affect body function [4]. In addition to regulating

specific target genes, miRNAs can modulate cellular functions by binding to promoters to activate transcription processes or directly activating receptor proteins [5]. Different miRNAs have different functions, and they can regulate multiple genes simultaneously or be regulated by multiple genes, which results in complex and diverse biological functions of miRNAs in organisms [6].

Previous studies have found that miRNAs affect the occurrence of cardiovascular diseases by regulating angiogenesis and apoptosis, and the underlying action mechanism is related to the inflammatory response and oxygen radical formation [7]. Some exosomal miRNAs derived from mesenchymal stem cells have been found to inhibit oxidative stress, protect the heart, and potentially treat cardiovascular diseases [8,9]. Reduction in I/R injury is essential for myocardial protection, complication reduction, and long-term improvement in patients' quality of life. Presently, no effective treatment exists for I/R injury, which can be alleviated only by enhancing cardiac function via drug administration, reducing myocardial metabolism at low temperatures, and employing ischemic preconditioning and postconditioning techniques [10].

miRNAs are closely associated with the pathogenesis of various diseases but their relationship with myocardial I/R injury remains unclear. In this study, we



aimed to explore the role and function of miRNAs and to identify the target genes regulating I/R. In medical research, high-throughput sequencing can provide complete genetic sequences of specific cells or tissues. Therefore, we used high-throughput sequencing to screen differentially expressed miRNAs and bioinformatics to analyze their potential functions. Additionally, we explored the relationship between significantly expressed *miR-200a-3p* and ferroptosis in the context of I/R injury, aiming to enhance our understanding of the underlying mechanism and guide future research.

## 2. Materials and Methods

### 2.1 Cell Culture and H/R Model Construction

The rat H9C2 myocardial cell line was obtained from the cell repository available at the Chinese Academy of Sciences. The stored myocardial cells were revived and prepared for passage. Cells in a healthy growth state after three cell passages were utilized for further experiments. Cell lines are regularly authenticated and tested for mycoplasma by the authors. The control group cells were treated with normal Dulbecco's modified Eagle's medium (DMEM) supplemented with 10% fetal bovine serum (FBS) and 1% antibiotics (Sigma-Aldrich, St. Louis, MO, USA). In contrast, the hypoxia/reoxygenation (H/R) model group cells were exposed to glucose-free DMEM to simulate anoxic conditions. An anoxic environment was created using a three-gas incubator (BD Biosciences, Franklin Lakes, NJ, USA) (anoxic conditions: 94% N<sub>2</sub> + 5% CO<sub>2</sub> + 1% O<sub>2</sub>). After 6 h, the medium was removed, and FBS and glucose were supplemented and placed in a sugar culture medium and normoxic incubator for reoxygenation for 16 h (normoxic conditions: 95% air + 5% CO<sub>2</sub>).

### 2.2 Apoptosis Detection

The cells designated for analysis were harvested, collected in phosphate-buffered saline, centrifuged, and washed thrice. Subsequently, 300  $\mu$ L of binding buffer (1 $\times$ ) (ServiceBio, Wuhan, China) was added to the tube. Reagents from the Annexin apoptosis detection kit (Gibco, Carlsbad, CA, USA) were added and mixed gently. Following an incubation period of 15 min in the dark, an additional 200  $\mu$ L of binding buffer (1 $\times$ ) was added, and the cells were analyzed using flow cytometry (ACEA Biosciences, San Diego, CA, USA).

### 2.3 High-Throughput Sequencing

#### 2.3.1 Extraction of Total RNA

RNA was extracted from rat H9C2 myocardial cells in the control group (normal group) and model group (hypoxia and reoxygenation groups), with three repeats. Total RNA Extractor Kit (Gibco) was used for RNA extraction. The solution was centrifuged after the addition of 200  $\mu$ L of chloroform. Subsequently, the pellet was washed with 75%

ethanol. After repeated centrifugation, the supernatant was dissolved in RNase-free ddH<sub>2</sub>O (Vazyme, Nanjing, China). Finally, the RNA concentration was tested for eligibility.

#### 2.3.2 Construction of miRNA Library

The total RNA was extracted to prepare the RNA mix, and T4 RNA ligase was used to connect the 3'/5' ends of RNA. The cDNA chain was formed using the cDNA Synthesis Kit (Vazyme) and amplified using polymerase chain reaction (PCR) to obtain the final library product [11]. The quality of the sequencing data of the samples was checked using FastQC software (V0.12, Babraham Institute, Cambridge, Britain). The reads and reference genomes were aligned and analyzed using Bowtie software (V2.0, Hopkins, Baltimore, MD, USA).

#### 2.3.3 Screening for Differentially Expressed miRNAs

The original data were filtered, and according to the characteristics of the miRNA, reads of length 17–35 nucleotides were retained to obtain clean data. We analyzed the known and novel miRNAs and standardized the read count data using various databases. edgeR was used to determine the differences for samples without biological duplication. However, a negative binomial distribution model was used to analyze the differences for samples with biological duplication, and DESeq2 was adopted for analysis. For differentially expressed genes, we set the screening criteria of  $p < 0.05$  and  $\log_2(\text{fold change})$  absolute value  $> 1$  [12] (**Supplementary Table 1**).

#### 2.4 Real-Time-Quantitative PCR

TRIzol Reagent (Gibco) was added to cells, and RNA was extracted using an extraction kit (Gibco). cDNA was synthesized from the extracted RNA using a reverse transcription kit (Gibco). The purity of miRNA was determined using an ultraviolet spectrophotometer (Bio-Rad, Hercules, CA, USA), and fluorescence-based quantitative PCR (qPCR) was performed using a real-time qPCR detection kit (Gibco) and a qPCR system (Bio-Rad). Relative gene expression was calculated using the  $2^{-\Delta\Delta C_t}$  method. The five most significant differentially expressed miRNAs were selected for qPCR. Primers were synthesized by Shanghai Bioengineering Company (Table 1).

#### 2.5 Cell Transfection and Grouping

The H9c2 cells with optimal growth were seeded onto the culture plate, and transfection was initiated at the appropriate cell density. Briefly, cells were transfected with the *miR-200a-3p* inhibitor and the inhibitor-negative control (NC) was the control. Cell transfection was performed using Opti-MEM (Invitrogen, Carlsbad, CA, USA) and Lipofectamine 3000 transfection reagent (Invitrogen). Inhibition was confirmed by qPCR analysis with the following primer sequences: *miR-200a-3p* inhibitor sequence: 5'-ACAUCGUUACCAGACAGUGUUA-

**Table 1. qPCR primer sequence.**

miRNA	Forward primer (5'-3')	Reverse primer (5'-3')
miR-153-3p	CGCGTTGCATAGTCACAAAA	AGTGCAGGGTCCGAGGTATT
miR-181b-1-3p	CGCGTCTACTGAACAATGA	AGTGCAGGGTCCGAGGTATT
miR-200a-3p	GCGCGTAACACTGTCTGGTAA	AGTGCAGGGTCCGAGGTATT
miR-222-5p	GCGGGCTCAGTAGCCAGT	AGTGCAGGGTCCGAGGTATT
miR-224-5p	CGCGCAAGTCACTAGTGGTT	AGTGCAGGGTCCGAGGTATT
U6	ATTGGAACGATACAGAGAAGATT	GGAACGCTTCACGAATTTG

qPCR, quantitative polymerase chain reaction; miRNA, microRNA.

3', *miR-200a-3p* inhibitor-NC sequence: 5'-UCUACUCUUUCUAGGAGGUUGUGA-3'. Following successful transfection, the cells were divided into model + *miR-200a-3p* inhibitor group and model + *miR-200a-3p* inhibitor-NC groups based on the transfection content.

### 2.6 Cell Viability, ROS Generation, and Iron Ion Measurement

The Cell Counting Kit-8 (CCK-8) assay (Sigma-Aldrich) was used to detect cell viability. Its principle is outlined as follows: in the presence of 1-Methoxy PMS, WST-8 can be reduced to produce the highly water-soluble orange formazan dye. The amount of formazan dye produced is proportional to the number of viable cells. A reactive oxygen species (ROS) assay kit (Sigma-Aldrich) was employed to detect intracellular ROS production. Dichlorodihydrofluorescein diacetate (DCFH-DA) has no auto-fluorescence and can freely cross the cell membrane. When ROS is present in the cell, DCFH is oxidized into a strong green fluorescent substance, and the fluorescence intensity indicates the level of ROS. Iron colorimetric and  $\text{Fe}^{2+}$  colorimetric assay kits (Sigma-Aldrich) were employed to detect intracellular  $\text{Fe}^{2+}$  and  $\text{Fe}^{3+}$ . The analysis is based on the principle that iron and proteins combine to form a complex, which dissociates under acidic conditions.

### 2.7 Western Blotting

Cell lysis buffer was added to the samples on ice. Subsequently, the samples were centrifuged for 10 min, with total proteins obtained after decanting the supernatant. The protein concentration was determined using a bicinchoninic acid kit (Gibco). The protein samples were subjected to SDS-PAGE on 10% gels for 1.5 h. The resolved proteins were transferred onto a polyvinylidene fluoride (PVDF) membrane (CWBIO, Taizhou, China) and sealed with sealing liquid (5% skimmed milk) for 90 min. The PVDF membrane was incubated with diluted primary antibodies and the corresponding secondary antibodies. Enhanced chemiluminescence solution (CWBIO) can emit light through chemical reactions, which was added dropwise onto the blotting membrane placed under a gel imaging system (ACEA Biosciences). The primary antibodies used were anti-GAPDH (HC301, 1/2000; TransGen Biotech, Beijing, China), anti-TFRC (AF5343,

1/1000; Affinity, Liyang, China), anti-ACSL4 (DF12141, 1/1000; Affinity), and anti-GPX4 (67763-1-Ig, 1/1000; Proteintech, Wuhan, China). The secondary antibody was horseradish peroxidase-conjugated goat anti-rabbit IgG (H+L) (GB23303, 1/2000; ServiceBio).

### 2.8 Statistical Analyses

SPSS 20.0 (IBM Corp., Armonk, NY, USA) software was used for statistical analyses. All experiments were repeated three times, and quantitative results are presented as mean  $\pm$  standard deviation. Quantitative comparisons between two groups and among multiple groups were performed using independent-sample *t*-test and one-way analysis of variance, respectively. Results were considered statistically significant at  $p < 0.05$ . Studies involving human and animal subjects are not included in the manuscript, and an ethics statement is not applicable. The institutional review boards at the First Hospital of Shanxi Medical University considered this study exempt.

## 3. Results

### 3.1 Growth and Apoptosis of H9C2 Myocardial Cells

The cells in the control group exhibited better growth, whereas noticeable structural damage, increased cell fragments, and a higher number of necrotic cells were observed in the model group than in the control group (Fig. 1a). The findings of apoptotic analysis were in line with the morphological observations, and the apoptotic rate of cells was significantly higher in the model group than in the control group ( $p < 0.05$ ) (Fig. 1b).

### 3.2 High-Throughput Sequencing

#### 3.2.1 Differential Expression of miRNAs

The control (Group A) and model (Group B) groups were analyzed with three replicates. We identified 113 differentially expressed miRNAs, of which 76 were upregulated, whereas 37 were downregulated. Among these, 41 were known miRNAs, and 72 were novel. A heat map has been used to classify genes and their relationships (Fig. 2a). A volcano plot has been used to show the significant difference and change in the extent of expression between the groups (Fig. 2b). The violin plot shows the miRNAs expression of each sample (Fig. 2c).

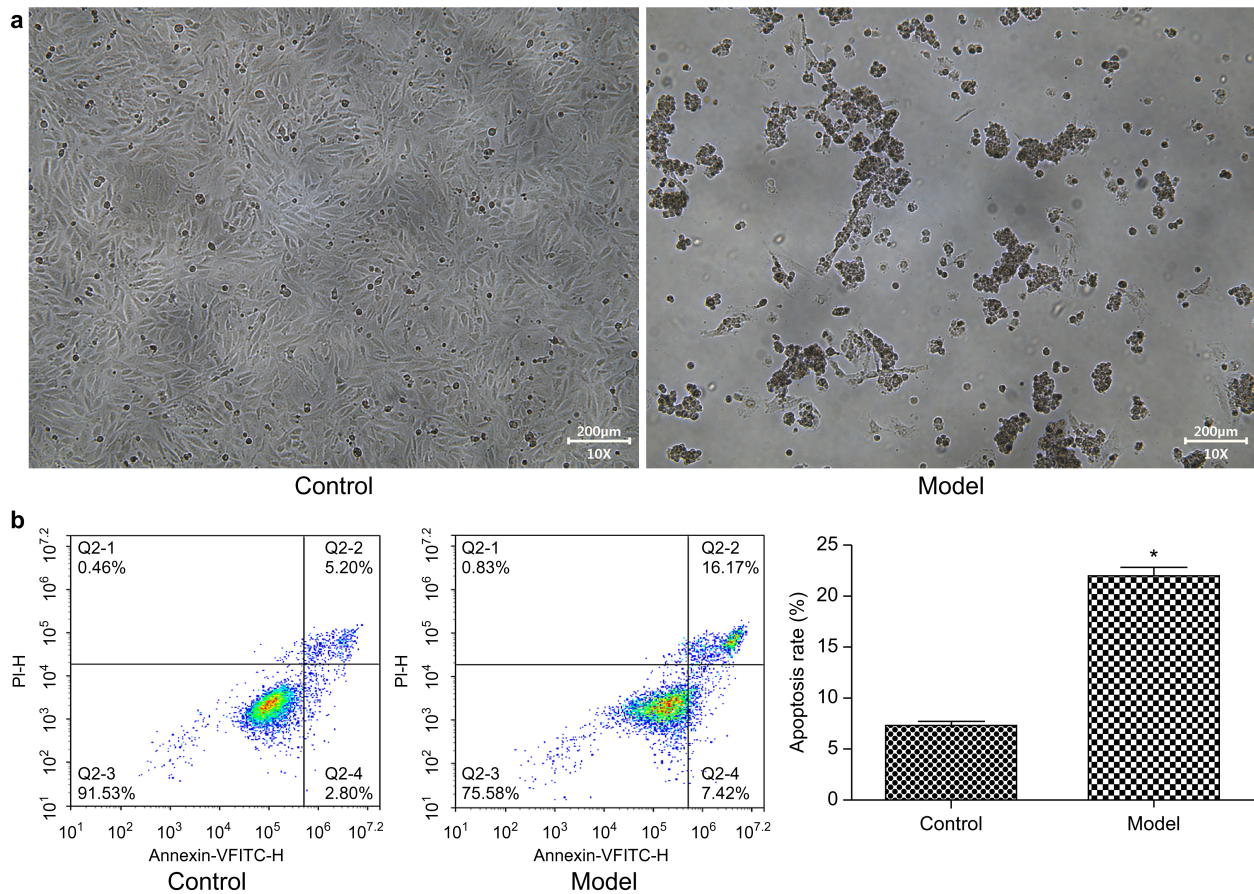


**Fig. 1. Myocardial cell growth and apoptosis.** (a) Microscopic observation of myocardial cell growth (100 $\times$ ). (b) Myocardial cell apoptosis was detected using flow cytometry. All experiments were repeated three times. \* $p < 0.05$  vs. control.

### 3.2.2 Functional Analysis of Differentially Expressed miRNAs

In the Gene Ontology (GO) term analysis, we ranked the functions of target genes from high to low, and their principal functions were pre-miRNA transcriptional regulation by RNA polymerase and promoter, transferase/protein kinase activity, negative regulation of signaling pathways, and intracellular signaling (Fig. 3a). In the Kyoto Encyclopedia of Genes and Genomes (KEGG) analysis, the top target genes played roles in amino acid metabolism, protein digestion and absorption, VEGF/MAPK signaling pathway, and apoptosis (Fig. 3b).

### 3.3 Verification of Differentially Expressed miRNAs Using qPCR

We selected five genes with the most notable variations in expression among the groups for qPCR verification from the recently identified miRNAs. The model group exhibited increased expression of *miR-153-3p* and *miR-200a-3p* than that in the control group. Conversely, a significant decrease in expression was observed for *miR-181b-1-3p*, *miR-222-5p*, and *miR-224-5p* in the model group ( $p < 0.05$ ) (Fig. 4a). The verification results aligned with the abovementioned predictions.

### 3.4 Verification of Transfection with *miR-200a-3p* Inhibitor Using qPCR

Based on predictions derived from the TargetScan (V8.0) and StarBase (V2.0) databases, it is suggested that the transferrin receptor (*TFRC*) could potentially serve as the target gene of *miR-200a-3p*. *TFRC* or *CD71*, is a type II transmembrane glycoprotein, mainly expressed on the surface of the cell membrane. As an important cytokine for iron uptake, *TFRC* is indispensable in the regulation of cellular iron transport and may affect I/R through the ferroptosis pathway [13]. To investigate this potential association, we modulated the expression of *miR-200a-3p*. The expression levels of *miR-200a-3p* in the four groups of myocardial cells were assessed using qPCR, thereby validating transfection efficiency. The results revealed higher levels of *miR-200a-3p* in the model group than in the control group. Additionally, a significant decrease in *miR-200a-3p* levels was observed in the inhibitor group compared with that in the model group ( $p < 0.05$ ). Notably, no significant difference was observed in *miR-200a-3p* levels between the inhibitor group and the inhibitor-NC group ( $p > 0.05$ ) (Fig. 4b). These findings indicate the successful transfection of the inhibitor into the cells, thereby substantiating its inhibitory effect.

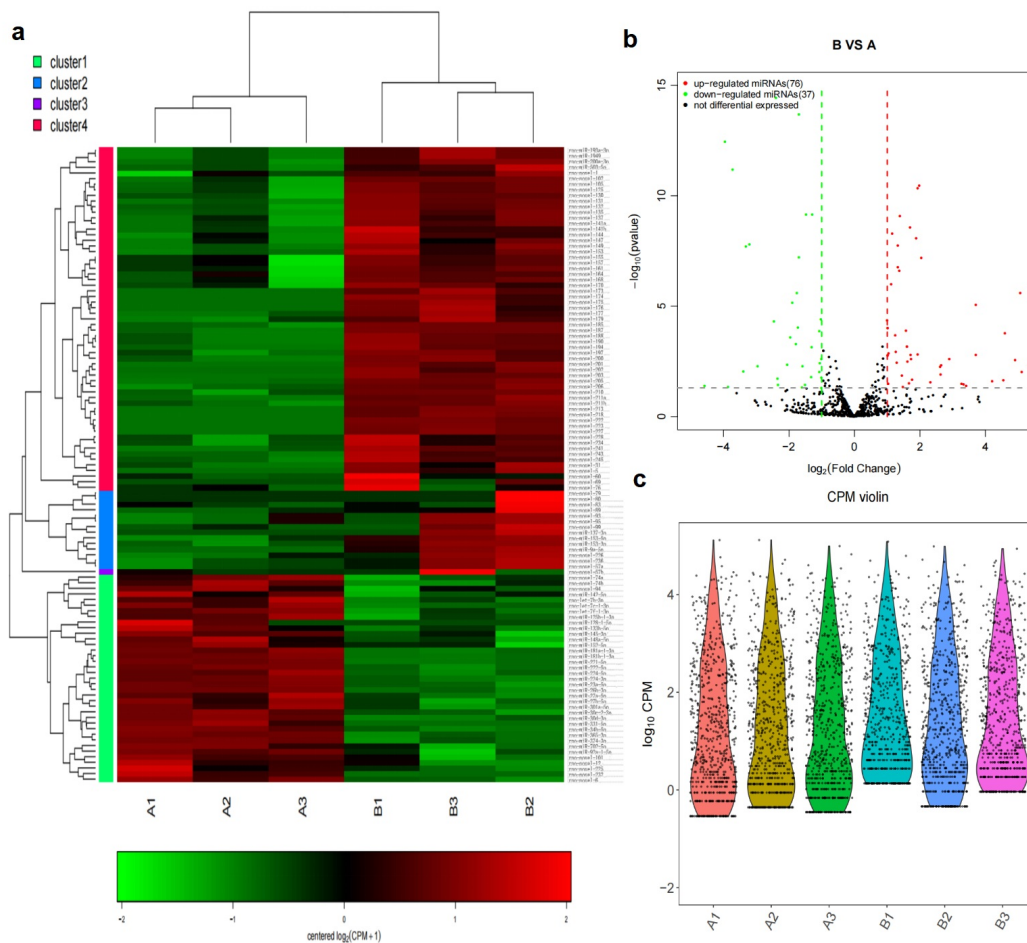


**Fig. 2. Results of differentially expressed miRNAs.** (a) Heat map. Heat map divided the genes into four clusters, showing the clustering relationship of different genes. Red parts represent high expression, and green parts represent low expression. (b) Volcano plot. The boundary is  $\log_2(\text{fold change})$  absolute value  $>1$ . Genes indicated in red, green, and black represent upregulated, downregulated, and without differential expression genes, respectively. (c) Violin plot. The X-axis shows the sample name, and the Y-axis presents the  $\log_{10}$  transformation value in CPM (read count per million).

### 3.5 Knockdown of *miR-200a-3p* Detects ROS Generation and Cell Viability

The levels of ROS were significantly higher in the model group than in the control group. Compared with that in the model group, ROS expression in the *miR-200a-3p* inhibitor group decreased, which reduced oxidative stress in the cells (Fig. 4c). Regarding cell viability, compared with the control group, the cell viability in the model group decreased significantly ( $p < 0.05$ ). Following inhibitor transfection, cell viability increased, indicating that the inhibition of *miR-200a-3p* could reduce cell damage (Fig. 4d).

### 3.6 Knockdown of *miR-200a-3p* Inhibits Ferroptosis

The analysis of iron ion levels revealed a significant increase in the model group than in the control group, indicating the occurrence of ferroptosis during I/R. Notably, inhibiting *miR-200a-3p* expression in the inhibitor group led to a substantial decrease in iron ion levels, demonstrat-

ing the role of *miR-200a-3p* in regulating iron ion levels (Fig. 5a). Western blot analysis further corroborated these findings. In the model group, the expression of *TFRC* and *ACSL4* exhibited an increase, whereas the expression of *GPX4* decreased compared to that in the control group. However, following inhibitor transfection, these ferroptosis markers displayed a contrasting pattern. Specifically, *TFRC* and *ACSL4* expression decreased, whereas *GPX4* expression increased within the inhibitor group. These results suggest a connection between *miR-200a-3p* expression levels and the occurrence of ferroptosis in cardiomyocytes (Fig. 5b,c).

## 4. Discussion

In this study, we used high-throughput sequencing technology to identify genes exhibiting differential expression in an H/R rat cardiomyocyte model. Experimental verification was conducted to validate our findings. Among

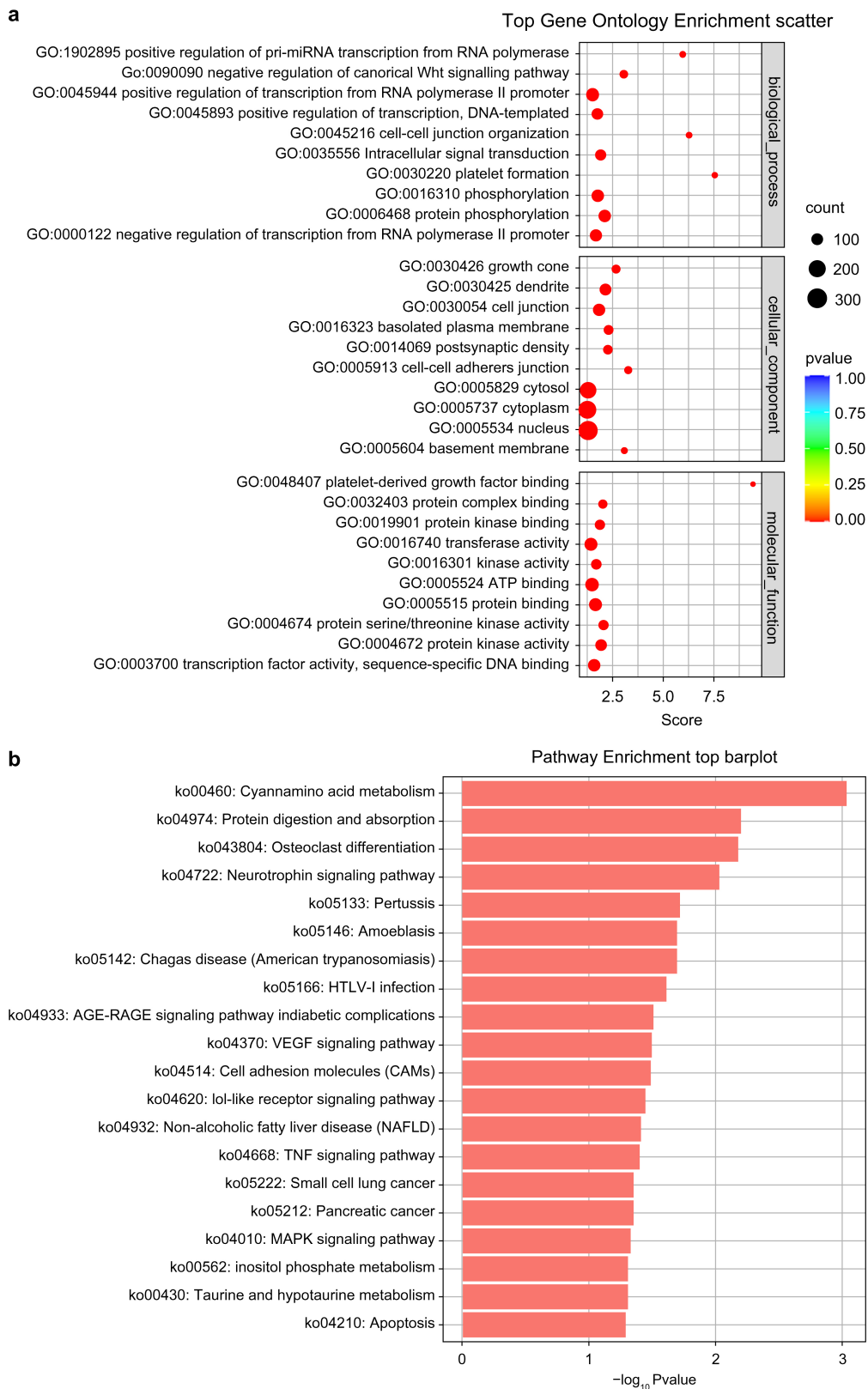


**Fig. 3. Functional analysis of differentially expressed miRNA target genes.** (a) Gene Ontology (GO) term enrichment. Bubble diagram, the horizontal coordinate represents the enrichment fraction. The left vertical coordinate represents the top 10 enriched functions in different regions. (b) Kyoto Encyclopedia of Genes and Genomes (KEGG) pathway enrichment. Bar graph, the horizontal coordinate represents the size of the statistical  $p$ -value. The vertical coordinate represents the biological information and signaling pathways.

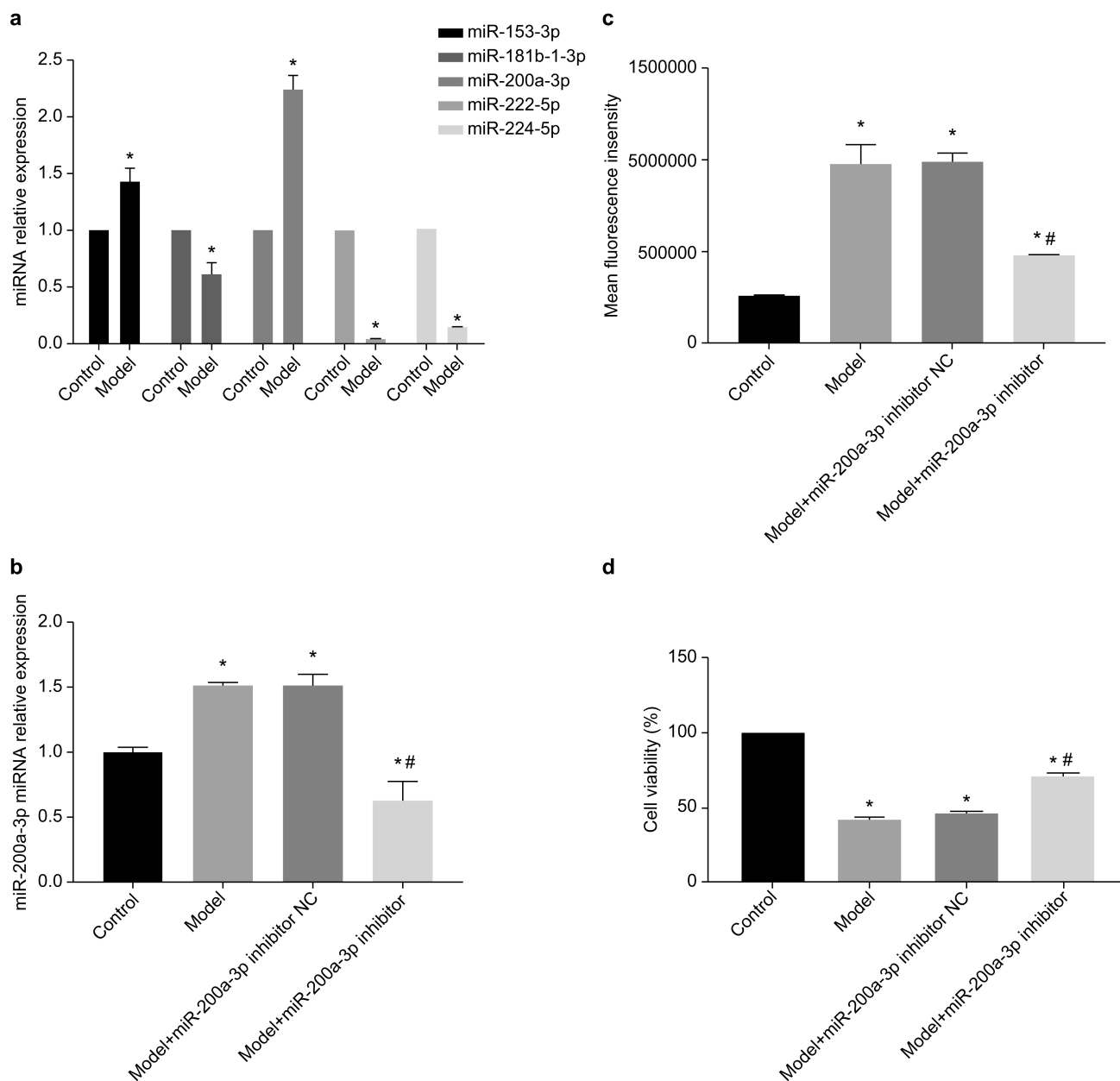


**Fig. 4. Analysis of differentially expressed miRNAs, reactive oxygen species (ROS), and viability in myocardial cells.** (a) miRNAs with differential expression were verified using qPCR. (b) The transfection efficiency of the *miR-200a-3p* inhibitor was verified using qPCR. (c) ROS levels in myocardial cells. (d) Cell viability in myocardial cells. All experiments were repeated three times. \* $p < 0.05$  vs. control, # $p < 0.05$  vs. model. NC, negative control.

the differentially expressed genes, *miR-200a-3p* stood out. To further investigate the role of *miR-200a-3p*, we assessed iron ion levels and ROS upon inhibiting *miR-200a-3p* while also evaluating the expression of iron death markers. These investigations suggest the potential involvement of *miR-200a-3p* in the ferroptosis pathway during I/R. The present study sheds light on novel avenues for modulating I/R injury and offers valuable insights for future research on prevention and treatment strategies.

miRNAs play essential roles in organisms and are among the most well-studied ncRNAs [14]. They are in-

involved in various life activities, including developmental process regulation, resistance to viral invasion, animal immune function regulation, and various systemic diseases and tumors [15]. In addition, miRNAs are associated closely with cardiovascular diseases. The levels of *miR-1* and *miR-499* levels increase in the blood of patients with myocardial infarction and have a specific reference value for disease diagnosis and prognosis. In heart failure, serum levels of *miR-132* and *miR-21* are associated with myocardial cell fibrosis and remodeling, and an increase in *miR-21* levels is positively correlated with an increase in *Gal-3*

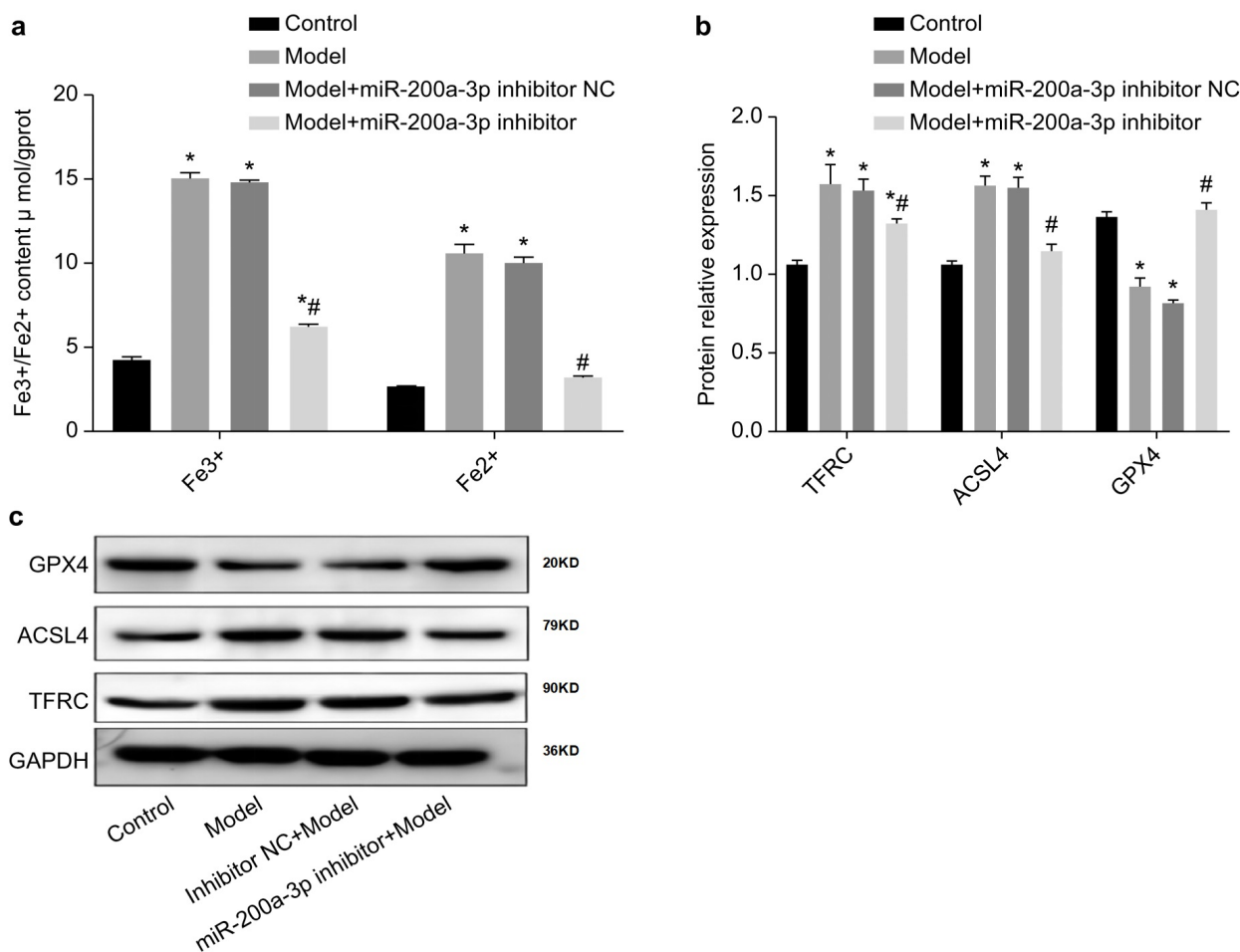


**Fig. 5. Analysis of the levels of iron ions and ferroptosis markers in myocardial cells.** (a) Iron ion levels in myocardial cells of the four groups. (b,c) Western blot showing the ferroptosis markers in the myocardial cells of the four groups. All experiments were repeated three times. \* $p < 0.05$  vs. control, # $p < 0.05$  vs. model.

levels [16,17]. Recent studies have demonstrated that *miR-200a-3p* reduces coronary microembolization in rats [18]. Coronary microembolization causes no or low reflux and aggravates the ischemic injury. The underlying mechanism is related to microvascular injury, microthrombus formation, and the release of various inflammatory and adhesion factors. Overall, miRNAs play important roles in disease development.

High-throughput sequencing, also called next-generation sequencing technology, distinguishes itself from the traditional dideoxy termination method by enabling the simultaneous detection of numerous molecules. It has found extensive applications across various disciplines. We identified 113 differentially expressed miRNAs in the control and model groups, comprising 76 upregulated and 37 downregulated genes, utilizing high-throughput sequencing. To explore the functions of these genes, we performed analyses using the GO and KEGG databases. Notably, we observed a significant increase in the expression of *miR-200a-3p*, a gene located

on chromosome 1 of the *miR-200* family. This gene has been implicated in cell differentiation, apoptosis, and tumor inhibition in previous research [19,20]. Furthermore, database prediction revealed a strong correlation between the expression of *miR-200a-3p* and genes such as *MCL1*, *CFL2*, and *TXNIP*. These genes are directly or indirectly involved in inflammatory responses, apoptosis, and tissue cell necrosis [21–23].

In the H/R model, we found that the levels of ROS were increased compared with those in the control. After inhibiting *miR-200a-3p* expression, ROS decreased significantly in the model group. Excessive ROS production poses a risk to the body. Since the heart has low levels of free radical scavenging mechanisms, excessive formation of ROS can easily lead to cardiovascular complications. It is an important mechanism underlying diabetes-associated inflammation and pathologic remodeling in the heart [24]. Cell ferroptosis, a novel cell death pathway, is implicated in various diseases. *TFRC*, a transferrin receptor, is responsible for the influx of iron ions into cells to promote ferroptosis.

Along with *GPX4* and *ACSL4*, *TFRC* has been confirmed as a marker for the regulation of ferroptosis [25]. Since the database predicts that *TFRC* is a target gene for *miR-200a-3p*, we hypothesized that *miR-200a-3p* could regulate MIRI by mediating ferroptosis via *TFRC*. Western blot showed that in the model group, the expression of *TFRC* and *ACSL4* exhibited an increase, whereas the expression of *GPX4* decreased compared to that in the control group. Upon inhibiting *miR-200a-3p*, the opposite was observed with respect to the expression of these markers. It indicated that ferroptosis occurred during H/R, which was related to *miR-200a-3p* levels. The experiment has shown that inhibiting *miR-200a-3p* expression could reduce ferroptosis and protect the myocardium. We plan to verify these relationships in experimental animal models in the future. The findings may provide a new direction for the treatment of MIRI.

The GO and KEGG enrichment analyses are two of the most commonly used methods in bioinformatics. They are used to study gene function by analyzing gene sequence and expression information [26,27] (**Supplementary Figs. 1,2**). The GO term enrichment analysis revealed that the gene functions are focused mainly on transcription factor regulation and related signal transduction. This finding is consistent with the functions of ncRNAs, which regulate downstream genes and influence protein synthesis. KEGG enrichment analysis predicted that the target genes are related to the VEGF, MAPK, and other signaling pathways. As a classical signaling pathway, the MAPK pathway regulates myocardial ischemia and ventricular remodeling and is implicated in cardiovascular diseases [28,29]. Dapagliflozin is a sodium-dependent glucose transporter-2 inhibitor that increases urinary sugar excretion by reducing the reabsorption of filtered glucose and lowering the renal glucose threshold. It also reduces the risk of cardiovascular events [30]. Dapagliflozin reduces myocardial injury and reperfusion arrhythmias through the MAPK signaling pathway induced via ferroptosis [31]. The expression of *miR-200a-3p* also inhibits ferroptosis in MIRI and plays a protective role in the myocardium, suggesting that *miR-200a-3p* is closely related to the MAPK pathway and cell ferroptosis, warranting further study.

Early diagnosis and treatment are essential for disease prevention, and the earlier the intervention is administered, the greater the benefits. As novel biomarkers, miRNAs are helpful for the early diagnosis of neoplastic diseases [32,33]. They play essential roles in cell differentiation and biological processes. Compared with traditional detection methods, a new generation of sequencing technology can predict gene expression and information faster and more accurately [34]. Further research on the underlying mechanisms and relationships between miRNAs and diseases using new technologies, such as miRNA chips, will improve our understanding of overall gene expression in living organisms, enabling the use of miRNAs as biomarkers for disease diagnosis. Moreover, it may open avenues for utilizing

miRNA molecules as drug targets or mimics in developing therapeutic interventions, providing a novel approach to treating human diseases [35].

This study has some limitations that warrant consideration. First, the samples sequenced were relatively small, and increasing the number of experimental samples can increase the accuracy of the results. Additionally, this study mainly involved *in vitro* analysis. Considering the differences between *in vivo* and *in vitro* experiments, more research on the *in vivo* mechanism underlying I/R is needed. In future studies, the association between miRNAs and related lncRNAs, along with the specific action pathways need to be explored as they may facilitate a better understanding of the disease [36,37].

## 5. Conclusions

We identified differentially expressed miRNAs using high-throughput sequencing and explored the functions of *miR-200a-3p*. Downregulation of *miR-200a-3p* expression inhibits ferroptosis and alleviates myocardial damage. These findings offer a novel perspective on I/R regulation; however, the specific mechanisms underlying the actions of *miR-200a-3p* require further study.

## Abbreviations

3'UTR, 3' Untranslated Region; DMEM, Dulbecco's modified Eagle's medium; FBS, Fetal bovine serum; PBS, phosphate-buffered saline; BCA, Bicinchoninic Acid; PVDF, Polyvinylidene fluoride; GO, Gene Ontology; KEGG, the Kyoto Encyclopedia of Genes and Genomes; RT-qPCR, Real Time-quantitative polymerase chain reaction; ROS, reactive oxygen species; H/R, hypoxia/reoxygenation.

## Availability of Data and Materials

The original contributions presented in the study are all included in the article/Supplementary Material. The datasets used and/or analysed during the current study are available from the corresponding author on reasonable request.

## Author Contributions

SL: Conceptualization, Data curation, Formal analysis, Investigation, Writing-original draft, Writing-review & editing. DL: Conceptualization, Investigation, Methodology, Writing-original draft, Writing-review & editing. YL: Project administration, Software, Writing-original draft, Writing-review & editing. YZ: Project administration, Software, Writing-review & editing. YJ: Conceptualization, Methodology, Project administration, Supervision, Writing-review & editing. All authors read and approved the final manuscript. All authors have participated sufficiently in the work and agreed to be accountable for all aspects of the work.

## Ethics Approval and Consent to Participate

Not applicable.

## Acknowledgment

Not applicable.

## Funding

This work was supported by grants from the Beijing Medical Award Foundation (grant number YXJL2021035306030) and Shanxi Provincial Key Research and Development Program (grant number 201803D31092).

## Conflict of Interest

The authors declare no conflict of interest.

## Supplementary Material

Supplementary material associated with this article can be found, in the online version, at <https://doi.org/10.31083/j.fbl2901038>.

## References

- [1] GBD 2019 Diseases and Injuries Collaborators. Global burden of 369 diseases and injuries in 204 countries and territories, 1990-2019: a systematic analysis for the Global Burden of Disease Study 2019. *Lancet* (London, England). 2020; 396: 1204–1222.
- [2] Samsky MD, Morrow DA, Proudfoot AG, Hochman JS, Thiele H, Rao SV. Cardiogenic Shock After Acute Myocardial Infarction: A Review. *JAMA*. 2021; 326: 1840–1850.
- [3] Beerkens FJ, Claessen BE, Mahan M, Gaudino MFL, Tam DY, Henriques JPS, *et al.* Contemporary coronary artery bypass graft surgery and subsequent percutaneous revascularization. *Nature Reviews. Cardiology*. 2022; 19: 195–208.
- [4] Barraclough JY, Joan M, Joglekar MV, Hardikar AA, Patel S. MicroRNAs as Prognostic Markers in Acute Coronary Syndrome Patients-A Systematic Review. *Cells*. 2019; 8: 1572.
- [5] He S, Valkov E, Cheloufi S, Murn J. The nexus between RNA-binding proteins and their effectors. *Nature Reviews. Genetics*. 2023; 24: 276–294.
- [6] DeVeale B, Swindlehurst-Chan J, Blesloch R. The roles of microRNAs in mouse development. *Nature Reviews. Genetics*. 2021; 22: 307–323.
- [7] Shah RV, Rong J, Larson MG, Yeri A, Ziegler O, Tanriverdi K, *et al.* Associations of Circulating Extracellular RNAs With Myocardial Remodeling and Heart Failure. *JAMA Cardiology*. 2018; 3: 871–876.
- [8] Guo Y, Yu Y, Hu S, Chen Y, Shen Z. The therapeutic potential of mesenchymal stem cells for cardiovascular diseases. *Cell Death & Disease*. 2020; 11: 349.
- [9] Nazari-Shafti TZ, Stamm C, Falk V, Emmert MY. Exosomes for Cardioprotection: Are We Ready for Clinical Translation? *European Heart Journal*. 2019; 40: 953–956.
- [10] Landoni G, Baiardo Redaelli M, Votta CD. Remote Ischemic Preconditioning and Cardiac Surgery. *The New England Journal of Medicine*. 2016; 374: 489.
- [11] Kozomara A, Griffiths-Jones S. miRBase: annotating high confidence microRNAs using deep sequencing data. *Nucleic Acids Research*. 2014; 42: D68–D73.
- [12] Bolger AM, Lohse M, Usadel B. Trimmomatic: a flexible trimmer for Illumina sequence data. *Bioinformatics* (Oxford, England). 2014; 30: 2114–2120.
- [13] Aisen P. Transferrin receptor 1. *The International Journal of Biochemistry & Cell Biology*. 2004; 36: 2137–2143.
- [14] Singh D, Rai V, Agrawal DK. Non-Coding RNAs in Regulating Plaque Progression and Remodeling of Extracellular Matrix in Atherosclerosis. *International Journal of Molecular Sciences*. 2022; 23: 13731.
- [15] Loganathan T, Doss C GP. Non-coding RNAs in human health and disease: potential function as biomarkers and therapeutic targets. *Functional & Integrative Genomics*. 2023; 23: 33.
- [16] Sygitowicz G, Maciejak-Jastrzębska A, Sitkiewicz D. MicroRNAs in the development of left ventricular remodeling and post-myocardial infarction heart failure. *Polish Archives of Internal Medicine*. 2020; 130: 59–65.
- [17] Wang Y, Liang Y, Zhao W, Fu G, Li Q, Min X, *et al.* Circulating miRNA-21 as a diagnostic biomarker in elderly patients with type 2 cardiorenal syndrome. *Scientific Reports*. 2020; 10: 4894.
- [18] Chen ZQ, Zhou Y, Chen F, Huang JW, Li HL, Li T, *et al.* miR-200a-3p Attenuates Coronary Microembolization-Induced Myocardial Injury in Rats by Inhibiting TXNIP/NLRP3-Mediated Cardiomyocyte Pyroptosis. *Frontiers in Cardiovascular Medicine*. 2021; 8: 693257.
- [19] Shadbad MA, Asadzadeh Z, Derakhshani A, Hosseinkhani N, Mokhtarzadeh A, Baghbanzadeh A, *et al.* A scoping review on the potentiality of PD-L1-inhibiting microRNAs in treating colorectal cancer: Toward single-cell sequencing-guided biocompatible-based delivery. *Biomedicine & Pharmacotherapy = Biomedecine & Pharmacotherapie*. 2021; 143: 112213.
- [20] Yin M, Chen WP, Yin XP, Tu JL, Hu N, Li ZY. LncRNA TUG1 Demethylated by TET2 Promotes NLRP3 Expression, Contributes to Cerebral Ischemia/Reperfusion Inflammatory Injury. *ASN Neuro*. 2021; 13: 17590914211003247.
- [21] Wang J, Wang XJ, Zhang Y, Shi WJ, Lei ZD, Jiao XY. TXNIP knockout improves cardiac function after myocardial infarction by promoting angiogenesis and reducing cardiomyocyte apoptosis. *Cardiovascular Diagnosis and Therapy*. 2022; 12: 289–304.
- [22] Wang S, Cheng Z, Chen X, Lu G, Zhu X, Xu G. CircUBXN7 mitigates H/R-induced cell apoptosis and inflammatory response through the miR-622-MCL1 axis. *American Journal of Translational Research*. 2021; 13: 8711–8727.
- [23] Nguyen K, Chau VQ, Mauro AG, Durrant D, Toldo S, Abbate A, *et al.* Hydrogen Sulfide Therapy Suppresses Cofilin-2 and Attenuates Ischemic Heart Failure in a Mouse Model of Myocardial Infarction. *Journal of Cardiovascular Pharmacology and Therapeutics*. 2020; 25: 472–483.
- [24] Marino F, Salerno N, Scalise M, Salerno L, Torella A, Molinaro C, *et al.* Streptozotocin-Induced Type 1 and 2 Diabetes Mellitus Mouse Models Show Different Functional, Cellular and Molecular Patterns of Diabetic Cardiomyopathy. *International Journal of Molecular Sciences*. 2023; 24: 1132.
- [25] Zheng S, Guan XY. Ferroptosis: Promising approach for cancer and cancer immunotherapy. *Cancer Letters*. 2023; 561: 216152.
- [26] Neely BA, Dorfer V, Martens L, Bludau I, Bouwmeester R, Degroove S, *et al.* Toward an Integrated Machine Learning Model of a Proteomics Experiment. *Journal of Proteome Research*. 2023; 22: 681–696.
- [27] Karp PD, Ivanova N, Krummenacker M, Kyrpides N, Latendresse M, Midford P, *et al.* A Comparison of Microbial Genome Web Portals. *Frontiers in Microbiology*. 2019; 10: 208.
- [28] Mollenhauer M, Bokredenghel S, Geißen S, Klinke A, Morstadt T, Torun M, *et al.* Stamp2 Protects From Maladaptive Structural Remodeling and Systolic Dysfunction in Post-Ischemic Hearts by Attenuating Neutrophil Activation. *Frontiers in Immunology*. 2021; 12: 701721.
- [29] Hall EJ, Pal S, Glennon MS, Shridhar P, Satterfield SL, Weber B, *et al.* Cardiac natriuretic peptide deficiency sensitizes the heart to

- stress-induced ventricular arrhythmias via impaired CREB signalling. *Cardiovascular Research*. 2022; 118: 2124–2138.
- [30] Inzucchi SE, Peixoto AJ, Testani JM. Glucose-Lowering Drugs to Reduce Cardiovascular Risk in Type 2 Diabetes. *The New England Journal of Medicine*. 2021; 385: 669–670.
- [31] Chen W, Zhang Y, Wang Z, Tan M, Lin J, Qian X, *et al*. Dapagliflozin alleviates myocardial ischemia/reperfusion injury by reducing ferroptosis *via* MAPK signaling inhibition. *Frontiers in Pharmacology*. 2023; 14: 1078205.
- [32] Miyoshi J, Zhu Z, Luo A, Toden S, Zhou X, Izumi D, *et al*. A microRNA-based liquid biopsy signature for the early detection of esophageal squamous cell carcinoma: a retrospective, prospective and multicenter study. *Molecular Cancer*. 2022; 21: 44.
- [33] Høgdall D, O'Rourke CJ, Larsen FO, Zarforoushan S, Christensen TD, Ghazal A, *et al*. Whole blood microRNAs capture systemic reprogramming and have diagnostic potential in patients with biliary tract cancer. *Journal of Hepatology*. 2022; 77: 1047–1058.
- [34] Green ED, Gunter C, Biesecker LG, Di Francesco V, Easter CL, Feingold EA, *et al*. Strategic vision for improving human health at The Forefront of Genomics. *Nature*. 2020; 586: 683–692.
- [35] Garcia-Martin R, Wang G, Brandão BB, Zanotto TM, Shah S, Kumar Patel S, *et al*. MicroRNA sequence codes for small extracellular vesicle release and cellular retention. *Nature*. 2022; 601: 446–451.
- [36] Abedpoor N, Taghian F, Hajibabaie F. Cross Brain-Gut Analysis Highlighted Hub Genes and LncRNA Networks Differentially Modified During Leucine Consumption and Endurance Exercise in Mice with Depression-Like Behaviors. *Molecular Neurobiology*. 2022; 59: 4106–4123.
- [37] Abedpoor N, Taghian F, Ghaedi K, Niktab I, Safaeinejad Z, Rabbiee F, *et al*. PPAR $\gamma$ /Pgc-1 $\alpha$ -Fndc5 pathway up-regulation in gastrocnemius and heart muscle of exercised, branched chain amino acid diet fed mice. *Nutrition & Metabolism*. 2018; 15: 59.